On-Orbit Calibration Assessment of NOAA-21 VIIRS Thermal Emissive Bands and Implications for JPSS-4 VIIRS

Amit Angal[a], Kwofu Chiang[a], Daniel Link[a], Carlos Perez Diaz[a],
Norvik Voskanian[b] , Kurt Thome[b]

[a] *Science Systems and Applications Inc, 10210 Greenbelt Rd, Lanham MD*
[b] *Sciences and Exploration Directorate, NASA Goddard Space Flight Center, Greenbelt, MD*

ABSTRACT

The Visible Infrared Imaging Radiometer Suite (VIIRS) instrument onboard the NOAA-21 (N21) satellite has been successfully operating for over three years collecting valuable scientific measurements. A large suite of weather forecasting models and scientific research applications are supported with the VIIRS measurements from N21 combined with those acquired from the VIIRS instrument onboard the S-NPP and NOAA-20 spacecraft. Among the 22 VIIRS spectral bands, there are seven thermal emissive bands (TEB) covering the 3.7 to 12.2 μm spectral range at two different spatial resolutions. The VIIRS TEB detectors are calibrated onboard using a blackbody at a controlled temperature and a space view for background signal measurement. In this paper, we discuss the on-orbit performance of the N21 VIIRS TEB using various parameters such as the detector gain, noise, and offset. This on-orbit assessment provides critical insights into instrument behavior and calibration performance that will inform pre-launch testing and post-launch validation strategies for the upcoming JPSS-4 VIIRS mission scheduled for launch in 2027. The methodologies and lessons learned from characterizing the N21 TEB performance will enable more efficient and comprehensive radiometric assessment of the next VIIRS instrument. Specific focus is placed on identifying performance trends and anomaly signatures observed during the N21 commissioning phase that can enhance the JPSS-4 instrument checkout procedures and accelerate the transition to routine on-orbit operations. The established performance baselines and uncertainty estimates will serve as an acceptance criterion for the JPSS-4 commissioning activities, ensuring mission readiness and data continuity for operational users.

1. INTRODUCTION

The Visible Infrared Imaging Radiometer Suite (VIIRS) is a critical environmental sensor providing global observations for weather forecasting, climate monitoring, and numerous scientific applications. The Joint Polar Satellite System (JPSS) program operates a constellation of VIIRS instruments aboard multiple satellites to ensure continuous data coverage.[1] NOAA-21 (N21) (also referred to as JPSS-2 or J2), launched on November 10, 2022, is the third operational VIIRS instrument following the successful Suomi National Polar-orbiting Partnership (S-NPP) launched in 2011 and NOAA-20 (JPSS-1) launched in 2017. With the upcoming launch of JPSS-4 (J4) scheduled for 2027, there is significant value in comprehensively documenting the early on-orbit performance of NOAA-21 VIIRS to inform pre-launch testing strategies and post-launch validation activities.

The VIIRS instrument features 22 spectral bands spanning from 0.41 to 12.2 μm, including seven thermal emissive bands (TEB) that cover the infrared spectral region from 3.7 to 12.2 μm. These TEB are designated as moderate-resolution bands M12, M13, M14, M15, and M16, along with imaging-resolution bands I4 and I5.[2] Table 1 summarizes the key characteristics of the VIIRS TEB, including their center wavelengths, spatial resolutions at nadir, and performance requirements. The spatial resolution varies between 375 m at nadir for the imaging bands and 750 m for the moderate resolution bands. Each TEB is required to meet stringent radiometric accuracy specifications with brightness temperature uncertainty requirements ranging from 0.4 K to 2.5 K depending on the band and scene temperature.[3,4]

Contact Author: Amit Angal (amit.a.angal@nasa.gov)

Table 1. VIIRS TEB design specifications. T_{typ}, typical temperature; Unc. Req., specified radiance uncertainty requirement in %.

FPA	Band	Spatial resolution at nadir (m)	Spectral range (μm)	Band Gain	T_{typ} (K)	Unc. Req. @ 190 K (%)	Unc. Req. @ 270 K (%)	Unc. Req. @ 310 K (%)
S/MWIR	**M12**	750	3.660–3.840	Single	270	-	0.7	0.7
	I4	375	3.550–3.930	Single	270	-	5.0	-
	M13	750	3.973–4.128	High	300	-	0.7	0.7
				Low	380	-	-	-
LWIR	**M14**	750	8.400–8.700	Single	270	12.3	0.6	0.4
	M15	750	10.263–11.263	Single	300	2.1	0.4	0.4
	I5	375	10.500–12.400	Single	210	-	2.5	-
	M16	750	11.538–12.488	Single	300	1.6	0.4	0.4

The primary objective of this paper is to provide a comprehensive assessment of the N21 VIIRS TEB on-orbit calibration performance, incorporating both prelaunch baseline characterization and operational behavior. By comparing the observed on-orbit performance against prelaunch expectations and examining trends relative to the heritage S-NPP and NOAA-20 instruments, we identify key lessons learned that will directly benefit J4 commissioning activities. This analysis focuses on critical calibration parameters including detector gain stability, noise equivalent temperature difference (NEdT), calibration coefficient trends from warm-up/cool-down (WUCD) observations, and the telemetry monitoring of onboard calibrator temperatures. Special emphasis is placed on identifying performance anomalies and trends during the N21 commissioning phase that can enhance J4 instrument checkout procedures and accelerate the transition to routine operations. Table 2 provides a summary of the key operational events on N21 VIIRS.

Table 2. Summary of the key operational events on N21 VIIRS

Key Operational Events
11/10/2022 - Launch
12/05/2022 - Nadir aperture door (NAD) open
02/08/2023 - Cryoradiator cooler door open
02/23/2023 - Mid-mission outgassing (MMOG #1)
03/03/2023 - CFPA set point change from 82 K to 80 K
03/10/2023 - Pitch Maneuver for RVS characterization
02/26/2024 - Mid-mission outgassing (MMOF #2)
06/22/2024 - Spacecraft safe mode
10/01/2025 - Spacecraft safe mode

This paper is organized as follows: Section 2 provides an overview of the VIIRS TEB calibration methodology, including the on-orbit calibration equation and prelaunch characterization approaches. Section 3 presents results from the telemetry trending analysis, including blackbody temperature and uniformity, focal plane array (FPA) temperature monitoring, and detector gain and noise performance. Section 4 summarizes key lessons learned for J4, and Section 5 provides concluding remarks.

2. METHODOLOGY

The VIIRS TEB calibration retrieves Earth View (EV) scene spectral radiance using a quadratic polynomial algorithm applied to background-subtracted detector responses combined with prelaunch-derived, instrument temperature-dependent calibration coefficients. The EV scene spectral radiance is retrieved via the following quadratic polynomial equation,

$$L_{EV} = \frac{F \cdot \sum_{i=0}^{2} c_i \cdot dn_{EV}^{i} - (RVS_{EV} - RVS_{SV}) \cdot \Delta L_{bg}}{RVS_{EV}}, \quad (1)$$

where ΔL_{bg} denotes the instrument background emission radiance difference, c_0 to c_2 are prelaunch-derived, instrument temperature-dependent calibration coefficients, dn_{EV} is the background-subtracted detector response for the EV scene, and RVS is the response versus scan angle at the EV and Space View (SV) angles of incidence. The radiances are further corrected for on-orbit detector degradation, instrument self-emission, and RVS effects. A key element of this algorithm is the F-factor — an on-orbit calibration scaling factor derived scan-by-scan by comparing the known onboard blackbody (BB) spectral radiance (as modeled thermally) against the radiance retrieved using prelaunch calibration coefficients. This F-factor effectively tracks and compensates for any on-orbit detector degradation. The instrument background emission term accounts for radiance contributions from the Rotating Telescope Assembly (RTA) and the Half-Angle Mirror (HAM) that do not cancel out in the path differences between the EV and SV angles.[4,5]

The onboard calibration blackbody (OBC BB) serves as the primary radiometric reference for TEB calibration. Its temperature is nominally controlled at 292.7 K and is derived from six thermistors embedded in the BB substrate, with a uniformity requirement of 30 mK. Periodically, BB warm-up and cool-down (WUCD) operations are performed during which the BB temperature cycles from instrument ambient to 315 K. These events serve to characterize changes in the TEB detector nonlinear responses, provide comprehensive noise characterization, as well as providing on-orbit derivations of the calibration coefficients (offset c_0, linear c_1, and nonlinear c_2). On-orbit WUCD-derived coefficients have been found to be largely consistent with these prelaunch LUT values, providing confidence in the stability of the instrument's radiometric response over its mission lifetime. [6,7,8]

Prelaunch characterization plays a critical role in the overall TEB calibration framework: the three quadratic calibration coefficients (c_0, c_1, c_2) used in the radiance retrieval algorithm are derived during prelaunch testing and stored as lookup tables (LUTs). The RVS was also characterized prelaunch using an external unpolarized source and was subsequently validated on-orbit via a dedicated spacecraft pitch maneuver performed during the early post-launch testing, showing agreement to within 0.4% between the prelaunch and on-orbit RVS values across most bands. [3,6]

The VIIRS TEB calibration uncertainty is computed by propagating the uncertainties inherent in the TEB measurements through to the Level 1B (L1B) radiance level using the standard error propagation formulation. Each contributing uncertainty source — including the radiance terms ($L_{BB}, L_{SV}, L_{EV}, L_{RTA}, L_{HAM}$), the calibration coefficients (c_0, c_1, c_2), the RVS, and the on-orbit detector response (dn_{EV}) — is characterized by its respective partial derivative with respect to the retrieved EV radiance, and each contribution is summed in quadrature to arrive at the total uncertainty. To avoid double-counting, uncertainties in the source path difference radiance are propagated into the calibration coefficient errors using the random measurement error and are not included again at the product-level error propagation. The resulting total uncertainty is evaluated for a single EV pixel across a range of scene temperatures and scan angles (beginning-of-scan, nadir, and end-of-scan), and the prelaunch-derived uncertainty LUTs are used as inputs to this algorithm. [9,10]

3. RESULTS AND DISCUSSIONS

This section presents the on-orbit calibration performance results for the N21 VIIRS TEB, spanning from launch in November 2022 through the current mission phase. The results are organized into three key areas: (1) telemetry trending, including onboard blackbody temperature and uniformity monitoring and cold FPA temperatures; (2) detector gain and noise performance, including band-averaged gain trends across key mission timeline periods and NEdT characterization; and (3) WUCD-derived calibration coefficient trending and total calibration uncertainty estimates.

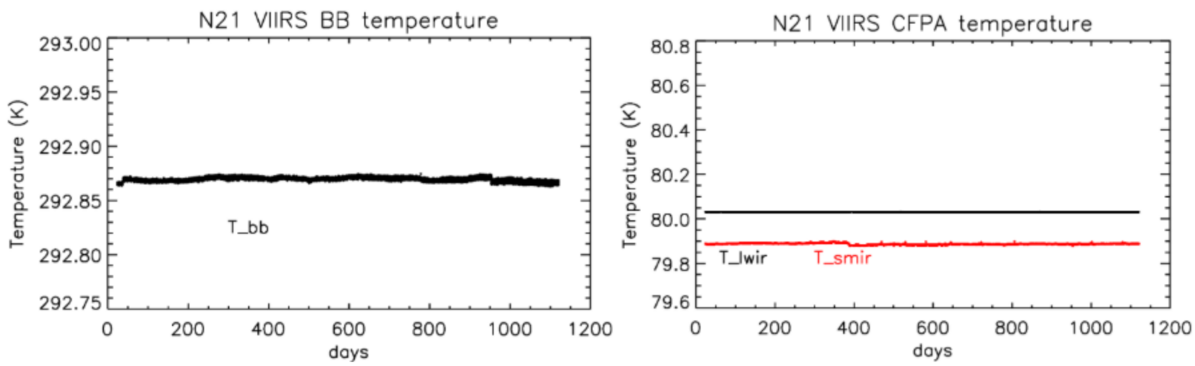

Figure 1. (left) Blackbody temperature trending and (right) CFPA temperatures for N21 VIIRS. (need an updated plot)

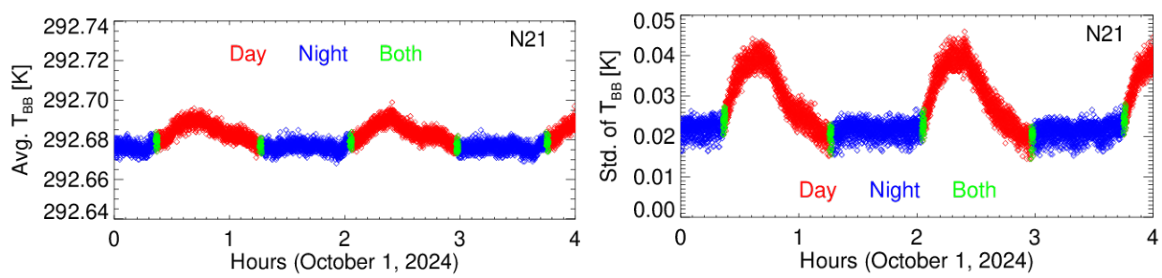

Figure 2. (left) Short-term trending of the blackbody temperature and (right) Standard deviation of the blackbody temperature.

Figures 1 and 2 show the N21 VIIRS OBC BB temperature and uniformity trends. Short-term BB temperature trending, over day and nighttime orbits, reveals orbital cycle variations with daytime variability exceeding the nighttime values and also the 30-mK specification — a non-compliance consistent with that observed during prelaunch characterization. Figure 1 (right panel) also presents the N21 CFPA temperature trends over the mission. The LWIR and S/MWIR FPA are cryogenically cooled to ~80 K, and their temperatures directly influence the prelaunch-derived calibration coefficients used in the radiance retrieval algorithm. Due to issues related to the thermal margin, the CFPA set point was changed from 82K to 80K shortly after launch - this triggered an update to the at-launch calibration LUTs.

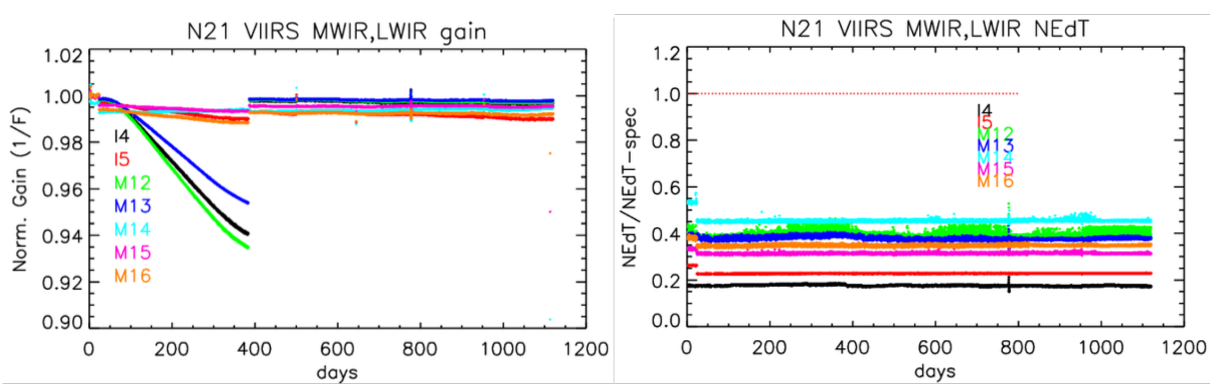

Figure 3. N21 VIIRS MWIR and LWIR (left panel) gain and (right) noise trends.

Figure 3 presents the NOAA-21 VIIRS TEB band-averaged detector gain (1/F-factor) trends for the MWIR and LWIR bands (left panel) and the corresponding band-averaged NEdT noise trends (right panel) from launch through the April 2026. The two mid-mission outgassing (MMOG) events — MMOG #1 on 23 February 2023 (day 105) and MMOG

#2 on 26 February 2024 (day 473) — are clearly identifiable as discontinuities in the gain trend time series. Both MMOG events were initiated in response to observed gain degradation in the detectors, attributed to ice contamination accumulating within the instrument dewar over time. The MMOG procedure involves controlled heating of the dewar assembly to sublimate the accumulated ice, after which detector responsivity is observed to recover toward its pre-degradation level. The gain trends are therefore best interpreted across three distinct timeline periods: before MMOG #1, after MMOG #1, and after MMOG #2, with each period reflecting a different state of detector responsivity relative to the onboard BB reference. Overall, the MWIR and LWIR bands exhibit good gain stability within each of the three timeline periods, and the NEdT values for all NOAA-21 TEB remain well within their respective specifications throughout the mission, consistent with the noise performance observed for the heritage S-NPP and NOAA-20 VIIRS instruments.

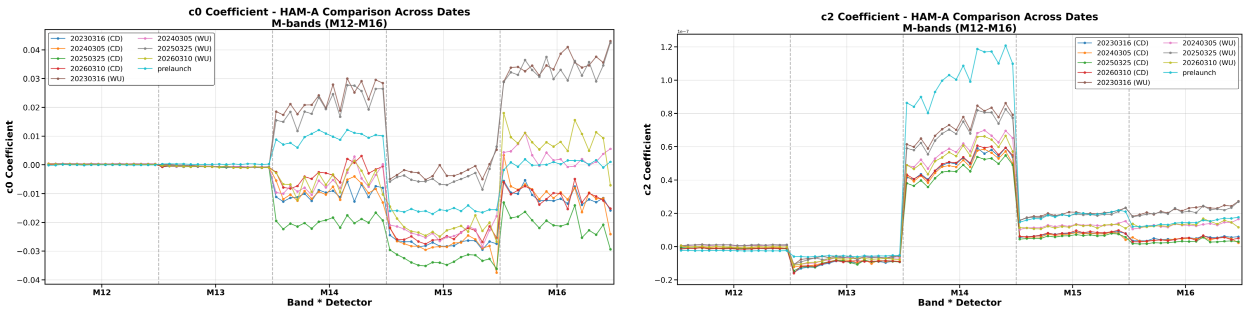

Figure 4. (left) c_0 and (right) $c_2$coefficients from prelaunch characterization and annual BB WUCD operations for the N21 VIIRS thermal moderate resolution bands.

Figure 4 presents the N21 VIIRS band-averaged on-orbit-derived calibration coefficients — the offset (c_0) and nonlinear (c_2) terms — for the moderate-resolution TEB (M12, M13, M14, M15, and M16), derived from each annual WUCD event since launch. Results are shown separately for the warm-up (WU) and cool-down (CD) sequences, with the prelaunch-derived LUT values included as a reference. The WUCD operation provides calibration coverage over a temperature range from instrument ambient (~267 K) to 315 K, enabling a robust second-order polynomial fit to the detector response as a function of incident BB radiance, from which the three coefficients are independently derived on-orbit. Overall, the on-orbit WUCD-derived coefficients for all moderate-resolution bands are found to be largely consistent with their prelaunch LUT, providing strong confidence in the stability of the N21 VIIRS TEB radiometric response. The offset (c_0) and nonlinear (c_2) coefficients are particularly stable across all completed WUCD events. Some differences between the WU and CD derived coefficients are noted, as the stepped nature of the WU temperature ramp tends to generate slightly larger nonlinear terms compared to the continuous, more seamless CD process. Any gradual trends in the linear coefficient (c_1), not shown here, for the MWIR bands M12 and M13 are consistent with the slow detector responsivity changes reflected in the F-factor gain trends shown in Figure 3.

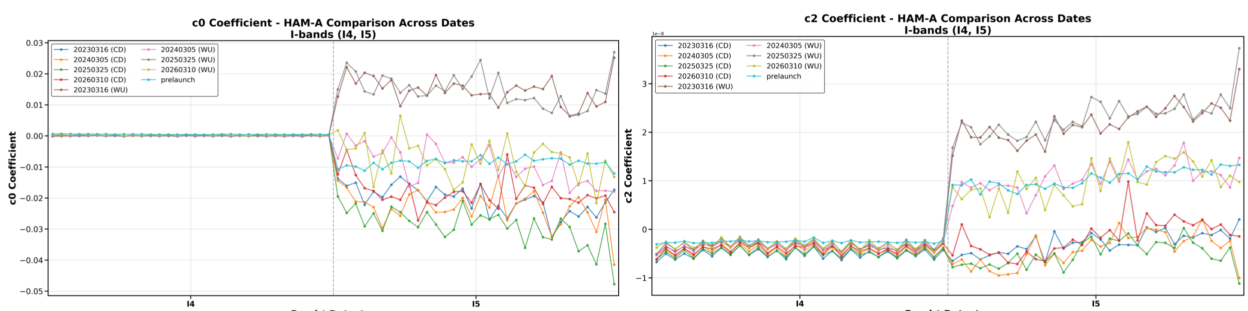

Figure 5. (left) c_0 and (right) $c_2$coefficients from prelaunch characterization and annual BB WUCD operations for the N21 VIIRS thermal imaging bands.

Figure 5 presents the corresponding on-orbit-derived calibration coefficients (c_0 and c_2) for the N21 VIIRS imaging-resolution TEB — bands I4 and I5 — again separated by WU and CD sequences and compared against prelaunch LUT reference values. Similar to the moderate-resolution bands, the imaging band coefficients derived from each

WUCD event are found to be in good agreement with the prelaunch characterization, demonstrating the stability of the detector nonlinear response for both the S/MWIR (I4) and LWIR (I5) bands. Taken together, Figures 4 and 5 confirm that the NOAA-21 VIIRS TEB prelaunch calibration coefficients remain valid representations of the on-orbit detector behavior, and that no significant changes in detector nonlinearity have occurred on-orbit. These results also establish a consistent calibration coefficient baseline that will serve as a valuable reference for the upcoming J4 VIIRS instrument during its post-launch commissioning activities.

Table 3. N21 VIIRS TEB total uncertainties compared with the specification in % of radiance at different scene temperatures. Non-compliances highlighted in red. M13 results are from high-gain stage.

TEB	Scene temperature [K] (Uncertainty spec., estimate)					
	190	*230*	*267*	*270*	*310*	*340*
I4	--	--	5.0, 2.4	--	--	--
I5	--	--	2.5, 0.30	--	--	--
M12	--	7.0, 11.10	--	0.7, 0.86	0.7, 0.22	0.7, 0.16
M13	--	5.7, 6.82	--	0.7, 0.66	0.7, 0.17	0.7, 0.13
M14	12.3, 1.73	2.4, 0.39	--	0.6, 0.17	0.4, 0.12	0.5, 0.11
M15	2.1, 0.63	0.6, 0.22	--	0.4, 0.12	0.4, 0.09	0.4, 0.08
M16	1.26, 0.51	0.45, 0.18	--	0.28, 0.10	0.26, 0.08	0.25, 0.07

Table 3 summarizes the NOAA-21 VIIRS TEB band-averaged total calibration uncertainties expressed as a percentage of retrieved radiance, evaluated at a range of scene temperatures (190 K, 230 K, 267 K, 270 K, 310 K, and 340 K) and compared against their respective specifications. Overall, the NOAA-21 VIIRS TEB demonstrate strong radiometric performance, with most bands well within their uncertainty specifications across most scene temperatures. The imaging bands I4 and I5 show estimated uncertainties of 2.4% and 0.30% at 267 K, respectively, both comfortably below their specifications of 5.0% and 2.5%. Among the moderate-resolution bands, the LWIR bands M14, M15, and M16 perform particularly well, with uncertainties well below 0.2% at scene temperatures of 270 K and above, and remaining compliant even at colder scenes of 190 K and 230 K — achieving values as low as 0.08% for M16 at 340 K compared to its specification of 0.25%. However, bands M12 and M13 exhibit non-compliance at lower scene temperatures: M12 reaches 11.10% at 230 K against a specification of 7.0%, and M13 reaches 6.82% against a specification of 5.7%, making these the only two bands that exceed their respective uncertainty requirements, a behavior that was also observed during the prelaunch characterization. With scene temperatures increasing to 270 K, M13 returns to compliance with an uncertainty of 0.66% against a 0.7% specification. Similarly, the band M12 uncertainty falls below specification for higher scene temperatures (310 K and above). This behavior at lower scene temperatures is consistent with results previously reported for S-NPP and NOAA-20 VIIRS, where the dominant uncertainty contributors for the MWIR bands at cold scenes are the onboard BB radiance and on-orbit detector response terms.

Table 4. N21 VIIRS TEB total uncertainties compared with the specification in degrees Kelvin at different scene temperatures. Non-compliances highlighted in red. M13 results are from high-gain stage.

TEB	Scene temperature [K] (Uncertainty spec., estimate)					
	190	*230*	*267*	*270*	*310*	*340*
I4	--	--	0.91, 0.43	--	--	--
I5	--	--	1.4, 0.17	--	--	--
M12	--	0.92, 1.35	--	0.13, 0.16	0.17, 0.05	0.21, 0.05
M13	--	0.85	--	0.14	0.19	0.23
M13	--	**0.93**	--	0.13	0.05	0.04
M14 spec.	0.65	0.24	--	0.14	0.12	0.13
M14	0.35	0.12	--	0.08	0.07	0.07
M15 spec.	0.56	0.24	--	0.22	0.28	0.34
M15	0.17	0.08	--	0.07	0.07	0.07
M16 spec.	0.48	0.26	--	0.24	0.31	0.37
M16	0.15	0.08	--	0.06	0.06	0.07

Table 4 presents the same total calibration uncertainties expressed in brightness temperature units (Kelvin), providing an intuitive measure of radiometric accuracy directly relevant to science users. The results are similarly encouraging, with nearly all bands meeting their temperature uncertainty specifications across the evaluated scene temperature range. The imaging bands I4 and I5 achieve uncertainties of 0.43 K and 0.17 K at 267 K, well below their respective specifications of 0.91 K and 1.4 K. For the moderate-resolution LWIR bands, M14, M15, and M16 all demonstrate very low temperature uncertainties, generally below 0.1 K at scene temperatures of 270 K and above, significantly outperforming their specifications — for example, M15 achieves 0.07 K at 270 K against a specification of 0.22 K, and M16 achieves 0.06 K against a specification of 0.24 K. At colder scenes (190 K and 230 K), the LWIR bands remain fully compliant, with M14 reaching 0.35 K at 190 K compared to its specification of 0.65 K. Bands M12 and M13 again exhibit the largest uncertainties at lower scene temperatures in temperature units as well, with M12 reaching 1.35 K at 230 K against a specification of 0.92 K and M13 reaching 0.93 K against a specification of 0.85 K — consistent with the radiance uncertainty non-compliance noted in Table 3. At warmer scene temperatures, both bands return to compliance, achieving uncertainties at or below 0.16 K and 0.13 K for M12 and M13 at 270 K, respectively. Taken together, the results from both tables confirm that the N21 VIIRS TEB calibration uncertainty performance is largely consistent with — and in many cases exceeds — the heritage performance of S-NPP and NOAA-20, with the known exception of bands M12 and M13 at colder scene temperatures.

4. LESSONS LEARNED

The on-orbit calibration performance assessment of N21 VIIRS presented in the preceding sections — encompassing BB telemetry trending, FPA temperature monitoring, detector gain and noise characterization, WUCD calibration coefficient analysis, and total calibration uncertainty estimates — collectively provides a comprehensive picture of the instrument's radiometric performance since launch. The observations and anomalies identified during the N21 commissioning phase, when viewed in the context of the heritage S-NPP and NOAA-20 VIIRS instruments, offer a unique and timely opportunity to extract actionable lessons learned that can directly inform the pre-launch testing, post-launch commissioning, and calibration validation strategies for the upcoming J4 VIIRS instrument, currently scheduled for launch in 2027. In the following section, we summarize the key lessons learned from the N21 TEB on-orbit experience and discuss their specific implications for J4 commissioning activities, with the goal of enabling a more efficient and accelerated transition to routine science operations for the next VIIRS instrument in the JPSS constellation.

4.1 Onboard Blackbody and Thermal Stability

One of the notable observations from the N21 commissioning phase was the identification of short-term BB uniformity non-compliance during early on-orbit operations. Unlike S-NPP and NOAA-20, the N21 BB exhibited periods where its temperature uniformity exceeded the 30-mK requirement, particularly during daytime orbital cycles. This behavior highlights the importance of closely monitoring BB temperature uniformity during J4's early post-launch phase and having mitigation strategies ready in advance. Additionally, thermal margin issues encountered during spacecraft (S/C) testing — related to the CFPA temperatures — underscore the need to carefully evaluate FPA thermal performance during J4 ground testing and to establish well-defined thermal margin criteria prior to launch. The N21 experience of requiring a CFPA set point change from 82 K to 80 K shortly after the cryoradiator cooler door open (approximately one month post-launch) is a particularly important lesson: J4 instrument checkout procedures should anticipate and plan for possible FPA set point adjustments and ensure that the calibration LUTs are updated accordingly in a timely manner.

4.2 Mid-Mission Outgassing and Gain Stability

As mentioned in Section 3, the N21 mission experienced two MMOG events, each of which produced observable changes in the TEB detector gain (1/F-factor) trends. Monitoring the gain behavior across these three distinct timeline periods (before MMOG #1, after MMOG #1, and after MMOG #2) has provided valuable insight into how outgassing events perturb detector responsivity and the time required to restabilize. For the J4 commissioning, it will be critical to schedule sufficient monitoring cadence around planned MMOG activities.

5. SUMMARY

This paper presents a comprehensive early on-orbit calibration assessment of the N21 VIIRS TEB, covering the period from launch in November 2022 through the current mission phase. The seven VIIRS TEB — spanning 3.7 to 12.2 µm across the moderate-resolution bands M12–M16 and imaging bands I4 and I5 — are calibrated on-orbit using the onboard calibration blackbody as the primary radiometric reference. An overview of the TEB calibration methodology is provided, including the quadratic polynomial radiance retrieval algorithm, prelaunch characterization of the calibration coefficients and RVS, and the standard error propagation formulation used to estimate total calibration uncertainty. Results from telemetry trending analysis — including BB temperature and uniformity, CFPA temperature monitoring, detector gain and noise characterization, and WUCD-derived calibration coefficient trends demonstrate that the N21 VIIRS TEB have been performing largely within their design specifications since launch, with notable observations including short-term BB uniformity non-compliance and gain changes associated with mid-mission outgassing events. Total calibration uncertainty estimates, evaluated across a range of scene temperatures and scan angles, show that most bands comply with their respective uncertainty requirements, consistent with the heritage performance of S-NPP and NOAA-20 VIIRS. The lessons learned from the N21 commissioning experience — particularly regarding the BB thermal stability and FPA set point adjustments and outgassing effects on detector gain — are discussed within the context of providing actionable recommendations to enhance the pre-launch testing and post-launch commissioning activities for the upcoming J4 VIIRS instrument.

ACKNOWLEDGEMENT

The authors would like to thank Xiaoxiong (Jack) Xiong, Jeff McIntire, and David Moyer for their invaluable contributions during the prelaunch and on-orbit calibration of the VIIRS instruments. In addition, the authors would also like to appreciate the efforts of the instrument vendor (Raytheon Technologies) during the successful test, integration, and commissioning of the VIIRS instruments.

REFERENCES

[1] L. Zhou, M. Divakarla, and X. Liu, "An overview of the joint polar satellite system (JPSS) science data product calibration and validation," Remote Sensing 8(2), 139 (2016).

[2] P. E. Ardanuy, C. F. Schueler, S. W. Miller, P. M. Kealy, S. A. Cota, M. Haas, and C. Welsch, "NPOESS VIIRS design process," Proc. SPIE 4483, 24–34 (2002).

[3] J. McIntire, D. Moyer, H. Oudrari, and X. Xiong, "Pre-launch radiometric characterization of JPSS-2 VIIRS thermal emissive bands," Remote Sensing 11(6), 732 (2019).

[4] X. Xiong, J. Butler, K. Chiang, B. Efremova, J. Fulbright, N. Lei, J. McIntire et al., "VIIRS on-orbit calibration methodology and performance," J. Geophys. Res. Atmos. 119(9), 5065–5078 (2014).

[5] B. Efremova, J. McIntire, D. Moyer, A. Wu, and X. Xiong, "S-NPP VIIRS thermal emissive bands on-orbit calibration and performance," J. Geophys. Res. Atmos. 119(18), 10859–10875 (2014).

[6] J. McIntire, D. Moyer, T. Chang, H. Oudrari, and X. Xiong, "Pre-launch JPSS-2 VIIRS response versus scan angle characterization," Remote Sensing 9(12), 1300 (2017).

[7] E. Johnson and C. Ranshaw, "VIIRS emissive band radiometric performance trending," Proc. SPIE 8510, 85101Y (2012).

[8] W. Wang, C. Cao, and S. Blonski, "NOAA-21 VIIRS thermal emissive bands early on-orbit calibration performance and improvements," IEEE Trans. Geosci. Remote Sens. 62, 1–13 (2024).

[9] C. P. Diaz, X. Xiong, Y. Li, and K. Chiang, "S-NPP VIIRS thermal emissive bands 10-year on-orbit calibration and performance," Remote Sensing 13(19), 3917 (2021).

[10] C. P. Diaz, K. V. Chiang, J. Sun, and X. Xiong, "VIIRS TEB calibration uncertainty analysis," Proc. SPIE 12264, 122640K (2022).